LANGMUIR Article
Cite This: Langmuir 2017, 33, 14263−14268
pubs.acs.org/Langmuir

Surface-Mediated Energy Transfer and Subsequent Photocatalytic Behavior in Silicon Carbide Colloid Solutions

David Beke,*[,†] Klaudia Horváth,[†] Katalin Kamarás,[†] and Adam Gali[†,‡]

[†]Institute for Solid State Physics and Optics, Wigner Research Centre for Physics, Hungarian Academy of Sciences, P.O. Box 49, H-1525 Budapest, Hungary

[‡]Department of Atomic Physics, Budapest University of Technology and Economics, Budafoki út 8, H-1111 Budapest, Hungary

Supporting Information

ABSTRACT: We demonstrate that particle−particle interaction affects the photocatalytic efficiency of colloids. Colloid silicon carbide nanoparticles were examined by varying their size, size distribution, and surface chemistry, and we found that surface moieties show no effect on the individual particles but dramatically affect the collective photocatalytic efficiency of the system.

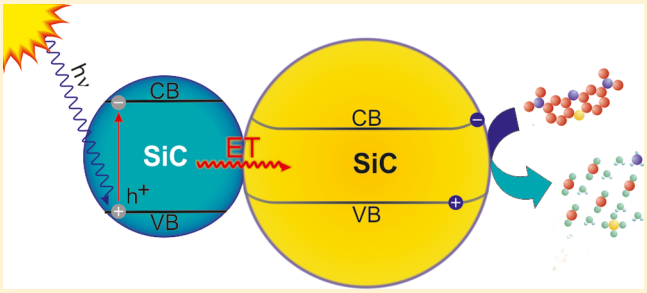

INTRODUCTION

Heterogeneous photocatalysts offer great potential for a variety of applications by converting photon energy into chemical energy.[1−3] However, finding the best material to catalyze photochemical reactions is strenuous owing to numerous factors that should be examined.[1,4] It has been inferred that the size and shape of a semiconductor particle play a major role concerning photocatalysis.[5,6] In bulk semiconductor photocatalysts, either holes or electrons are available for reaction because of band bending. However, in colloid semiconductor particle suspensions, electrons and holes may simultaneously be present on the surface, allowing several reaction routes. Decreasing the average particle size increases the number of surface sites available for charge transfer, while the rate of charge recombination also increases.[7,8] Further decrease in size, however, induces changes in the physical properties, too. When the spatial dimensions of the material are comparable to the de Broglie wavelength of carriers, quantum confinement leads to a transition from continuous to discrete energy levels that could significantly affect the photocatalytic activity. The gap between the occupied and empty energy levels increases, yielding a larger redox potential that, together with an unchanged solvent reorganization free energy, is expected to increase the photocatalytic activity.[7,9] However, contradictory results are often reported.[5,6,9,10] The inconsistency in the literature highlights the complexity of the particle behavior with size close to the exciton Bohr radius. Physical properties are no longer independent of the particle size, raising the importance of size distribution as the system may contain particles with various photocatalytic efficiencies. Usually, only the collective behavior can be monitored. As a result, unexpected differences in materials properties, that is, size distribution, size-dependent surface chemistry, and so forth, can lead to dramatic changes in the collective properties, that is, photocatalytic efficiency. Colloids are often described as uniformly dispersed particles in a continuous phase neglecting particle−particle interactions. However, dissipative structures are observed in many real systems.[11] The interaction between particles having the same composition but different photocatalytic properties, that is, slightly different band structures or charge affinity, or different shapes, can lead to the temporary formation of heterostructures or composites, and such assemblies can show photocatalytic behavior distinct from the individual particles. Surface chemistry may play a major role in this process that can control the interaction of nanoparticles (NPs). Tuning the surface chemistry to form NP ensembles can lead to significant changes in the overall properties without modifying the behavior of the individual particles.

By studying semiconductor NPs in the quantum confinement regime where size has a huge impact on the photocatalytic properties, we found that surface moieties regulate the interaction between the NPs in solution that results in the size-distribution-dependent photocatalytic activity. We used silicon carbide (SiC) as a model material. We found that particles with a diameter just above twice the exciton Bohr radius ($2a_B$) have significant photocatalytic efficiency comparable to ZnS, but SiC NPs with a diameter below $2a_B$ show negligible activity. However, such molecular-sized SiC NPs can enhance the efficiency of the larger particles, demonstrating the importance of size distribution. We find that this effect can be regulated by the surface chemistry of the NPs.

Received: October 2, 2017
Revised: November 23, 2017
Published: November 24, 2017

DOI: 10.1021/acs.langmuir.7b03433
Langmuir 2017, 33, 14263−14268

SiC is a chemically inert and biocompatible wide band gap semiconductor that has intermittently been investigated as a photocatalytic material candidate to generate organic fuels from CO_2,[12,13] to promote photoreduction, to produce hydrogen from water,[14−17] or to decompose organic pollutants,[18,19] making it eligible for our experiment. A study on electrochemical hydrogen evolution using SiC NPs showed[20] that thin films containing SiC NPs in the range of 3−8 nm have exceedingly high efficiency when used for water splitting, while larger particles (20 nm) show negligible effect. The sensitizer property of SiC NPs with a diameter of about 4 nm was studied on ZnS/SiC heterostructures.[21] SiC NPs enhanced the photocatalytic efficiency of ZnS as demonstrated in a dye degradation study. Recently, it was shown that the optical properties of SiC NPs drastically change at around 4 nm[22] with respect to those with the larger size. These findings, together with the mentioned size-dependent photocatalytic activity, prove that the photocatalytic efficiency of SiC is extremely size-dependent. Despite the suitable band gap position for water splitting, even for cubic type of SiC with a band gap as small as 2.3 eV, SiC as a photocatalyst is far from being understood.[23−25]

On the other hand, molecular-sized SiC NPs are exceedingly promising candidates to realize bioinert nonperturbative fluorescent NPs for in vivo bioimaging and sensing,[26−29] and the photocatalytic property of a label for bioimaging may affect its viability. Unwanted photoactivity of a NP can lead to phototoxicity,[30] while at the right place, phototoxicity can promote microbe disinfection, including antibiotic-resistant bacteria,[31] and kill cancer cells with photodynamic therapy.[31−33] Thus, examination of the photocatalytic behavior of the molecular-sized SiC NPs is of immediate importance when it is applied as a fluorescent biomarker.

EXPERIMENTAL SECTION

SiC NPs were prepared by stain etching[22,34] using 10 g of SiC powder. This solution has a broad size distribution (as-prepared). To study the photocatalytic efficiency of SiC NPs as a function of size, we used membrane separation to make two fractions from the as-prepared sample. Using a 30 kDa centrifuge filter (Pall, Macrosep), we can differentiate the NPs by size. NPs with diameters below $2a_B$ (1−4 nm, SiC-I) were collected, and the retentate contained the particles larger than 4 nm (4−16 nm, SiC-II). Detailed description of size separation as well as the results of further characterizations can be found in the Supporting Information. The size distribution of NPs was characterized by atomic force microscopy (Figure 1A). Besides NP size, surface states also affect the photocatalytic efficiency. Surface terminations of SiC NPs were measured by Fourier transform infrared (FTIR) spectroscopy, and we found no difference between the infrared-active moieties on SiC-I and SiC-II samples (Figure 1B).

The photocatalytic activity of different NPs was evaluated by the degradation of methylene blue (MB) under UV illumination. MB is a model cationic dye employed by industries such as textile industry for a variety of purposes. The reaction route during photocatalytic degradation is often unknown. Nevertheless, it is proposed that the photocatalytic degradation pathway of MB in water is a continuous oxidation process where hydroxylation leads to aromatic ring opening and subsequent mineralization.[37] When a photon with energy equal to or larger than the semiconductors band gap is absorbed, an electron−hole pair, that is, an exciton, is generated. The oxidation of MB can be due to the direct reaction with the holes; however, the oxidizing reagent is most likely molecular oxygen in its radical form that is formed when either the excited electron reacts with the dissolved oxygen or the hole reacts with a water molecule.

A catalyst (0.5 mg/mL) was used in a 6.3×10^{-6} M MB solution. For excitation, we used artificial light from a 450 W Xe lamp of a spectrofluorometer in the 310−350 nm wavelength range. The absorption of MB between 300 and 450 nm is low, whereas SiC-I NPs have an absorption peak at about 320−340 nm. Therefore, we can both eliminate self-photodegradation and maximize photon efficiency by applying photoexcitation in the wavelength region of 310−350 nm. The solutions were kept overnight in the dark before illumination. To make our results comparable with the literature data, we synthesized ZnS NPs and a ZnS/SiC NP composite according to ref 21 using 10 mL of SiC-I solution for the ZnS/SiC composite. The average size of ZnS NPs is 3.5 nm; however, they form aggregates with about 100 nm diameter.[21] Figure 2A,B represents ultraviolet−visible (UV−vis) absorption spectra of MB solution as a function of time over SiC-I and SiC-II NPs under illumination, respectively. MB has a characteristic absorbance in the 600−700 nm range and SiC NPs in the wavelength range below 300 nm. As can be seen, SiC-I NPs have higher absorbance than SiC-II.[22]

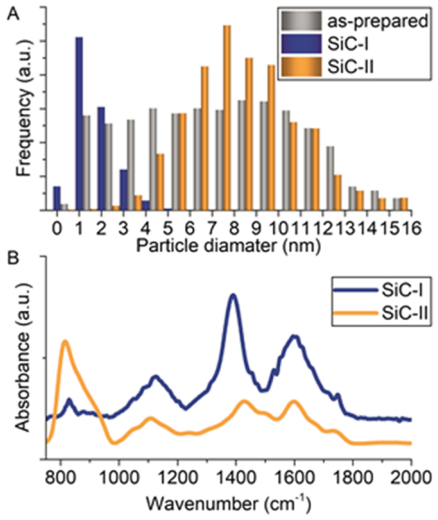

Figure 1. (A) Size distribution of as-prepared SiC, SiC-I, and SiC-II. (B) Infrared spectra of SiC-I and SiC-II. Spectra were taken by attenuated total reflectance and converted to absorbance. The main difference shows up as a peak at around 800 cm^{-1} that corresponds to SiC longitudinal optical (LO) phonon modes. The intensity of the LO mode is known to decrease in small SiC particles.[35,36]

RESULTS AND DISCUSSION

Degradation kinetics was measured as a change over time in the absorption band of MB at 663 nm. Figure 2C depicts the MB absorbance ratio (C/C_0) versus illumination time, where C and C_0 denote the characteristic absorption of MB after and before irradiation, respectively. As can be seen, the as-prepared SiC has a photocatalytic efficiency comparable to the ZnS/SiC composite studied before.[21] SiC-II is also able to degrade MB, but the efficiency is much lower. Interestingly, the SiC-I solution, which contains molecular-sized SiC NPs only, does not show any measurable photocatalytic activity, as MB absorbance in SiC-I is identical to that of the control sample (MB without catalyst). As the surface termination of SiC-I and SiC-II is the same inferred from FTIR, we conclude that size differences and variation in size distributions are responsible for the variety in photocatalytic activity of SiC-only samples. We identified both samples as SiC NPs (see Supporting Information). We note here that it is proposed that electrochemical etching of SiC can produce carbon fluorooxide (CFO) particles, too, with about 1−2 nm in size.[38] We use stain etching for the preparation of SiC NPs. The chemical dissolution mechanism during pore formation is usually described similarly; however, we recently proposed a no-

DOI: 10.1021/acs.langmuir.7b03433
Langmuir 2017, 33, 14263−14268

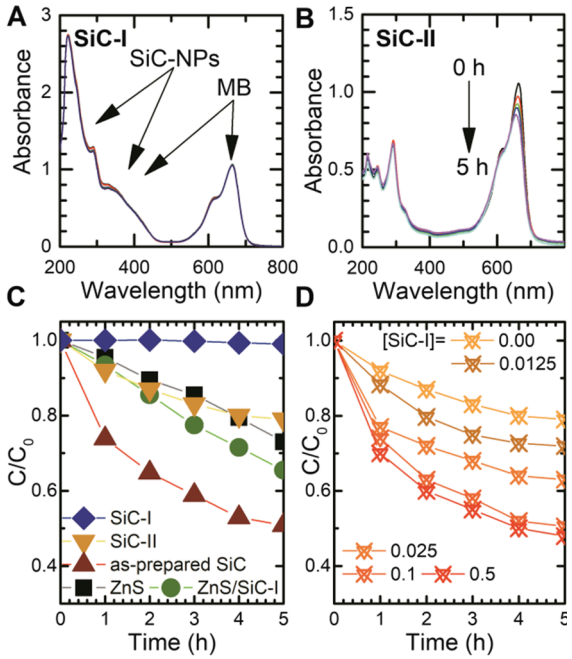

Figure 2. (A,B) UV−vis absorption spectra of MB solution as a function of time over SiC NPs with different sizes under UV illumination. We marked the particular absorption range of SiC-I and MB. (C) Plot of MB concentration ratio C/C_0 vs illumination time over various photocatalysts. (D) Plot of MB concentration ratio C/C_0 vs illumination time over increasing concentration of SiC-I (mg/mL) in 0.5 mg/mL solution of SiC-II.

photon exciton generation model to describe stain etching processes, which describe the stain etching mechanism differently.[39] Nevertheless, we cannot entirely exclude that CFO NPs might be present in SiC-I samples.

The result shows that size distribution significantly affects the photocatalytic efficiency of SiC NPs. Therefore, we studied the effect of size distribution by maintaining the concentration of SiC-II at a constant value (0.5 mg/mL), whereas the concentration of SiC-I particles was increased from 0.0125 to 0.5 mg/mL and measured the photocatalytic efficiency of the prepared systems. It can be seen in Figure 2D that the photocatalytic efficiency increases with the growth of the SiC-I concentration. We probably reach the efficiency maximum at 0.5 mg/mL as further increase has no detectable effect.

This result implies that the molecular-sized SiC NPs act as sensitizers for larger SiC NPs. Similar sensitizing effect was found for ZnS/SiC colloids (Figure 2). SiC NPs smaller than 4 nm have increased absorbance and luminescence quantum yield compared to the bulk material that has negligible luminescence as a result of its indirect band gap. The reported 1−10 ns decay times for SiC-I,[40] however, imply a fast carrier recombination rate and explain the negligible photocatalytic efficiency of SiC-I. By contrast, larger NPs (SiC-II) have bulklike optical properties[22] and exhibit longer carrier lifetime, although with an increased absorption efficiency compared to bulk SiC because of the relaxation of the optical selection rules, caused by the surface and other imperfections of the NPs. As a result, the higher absorption coefficient of SiC-I explains the detected sensitizing effect plausibly. However, such a mechanism needs particle−particle interaction at least during excitation which is rare in a stable colloid solution.

Indeed, NPs were easily fractioned by size using membrane filtration. Photocatalytic sensitizers act through energy transfer (ET) that requires close proximity of the sensitizer and the sensitized particles. Nevertheless, taking ET under examination, molecular-sized SiC NPs (SiC-I) can be excited in a relatively narrow wavelength range with a maximum at around 320 nm. Above 370 nm excitation, the photoluminescence intensity of SiC-I solution is negligible. Therefore, the expected ET can be verified through the wavelength-dependent photocatalytic efficiency study and by measuring the photoluminescence quenching of SiC-I NPs also in the presence of SiC-II NPs.

We illuminated the mixed solution that contains an equal amount of SiC-I and SiC-II particles (0.5 mg/mL), which showed the best photocatalytic efficiency, in the 360−400 nm region, where only SiC-II particles are excited, to check whether excitation of SiC-I particles is the key of the efficiency enhancement of SiC-II particles. The photocatalytic efficiency of the solution, in this case, decreased back to the efficiency of the pure SiC-II solutions. This experiment verifies that the excitation of the small particles is needed for the photocatalytic enhancement of the larger particles as the photocatalytic efficiency of pure SiC-II solution was wavelength independent in this optical excitation region.

To further study the ET mechanism, we maintained the concentration of the SiC-I constant, whereas the SiC-II concentration was increased. We recorded the emission spectra of SiC-I over different amounts of SiC-II under 320 nm excitation. Figure 3A shows that the addition of SiC-II

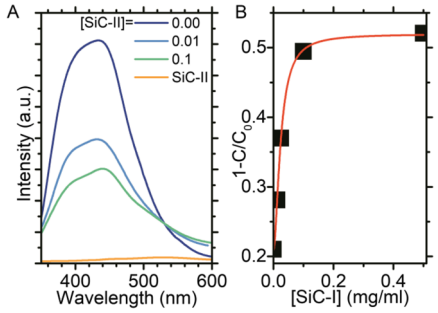

Figure 3. (A) Luminescence quenching effect. SiC-I concentration was maintained at 0.5 mg/mL, whereas the SiC-II concentration was increased. The orange curve is the very weak emission spectrum of pure SiC-II NPs. The excitation wavelength was 320 nm. (B) Photocatalytic efficiency ($1 - C/C_0$) vs SiC-I concentration (mg/mL). The plot is fitted with a Langmuir−Freundlich adsorption sigmoidal function.

decreases the luminescence intensity of SiC-I. In parallel, the weak SiC-II-related emission slightly increased compared to the pure SiC-II solution with the same concentration.

Both the wavelength-dependent photocatalytic efficiency study and the quenching of SiC-I luminescence implies ET between the molecular-sized SiC NPs and the larger SiC NPs. The plot of the photocatalytic efficiency as a function of SiC-I concentration shows a bimodal distribution, and it can be fitted well with a simple Langmuir adsorption model (Figure 3B). Both previous results[21] and the convergence of the efficiency indicate that SiC-I particles adsorb on the surface of SiC-II particles, and the efficiency increases till the maximal possible coverage is reached. Indeed, the particle−particle interaction can explain the measured ET in a colloid solution and its concentration dependency. Both resonant ET[41,42] and Dexter

DOI: 10.1021/acs.langmuir.7b03433
Langmuir 2017, 33, 14263−14268

electron transfer[43,44] are well-known for semiconductor quantum dots. Quantum confinement results in the enlargement of the gap between occupied and empty energy levels when the size of a semiconductor particle is reduced below the exciton Bohr radius. SiC-I particles show luminescence, and the energy of the emitted photon is about 2.75 eV (450 nm)[34] (see Figure 3A). The band gap of SiC-II is close to that of bulk SiC (2.34 eV, i.e., 530 nm).[22] Thus, particle−particle interaction leads to type I-like junction for proximate particles with different sizes similar to semiconductor composites or heterojunctions (see Figure 4). However, this type I junction

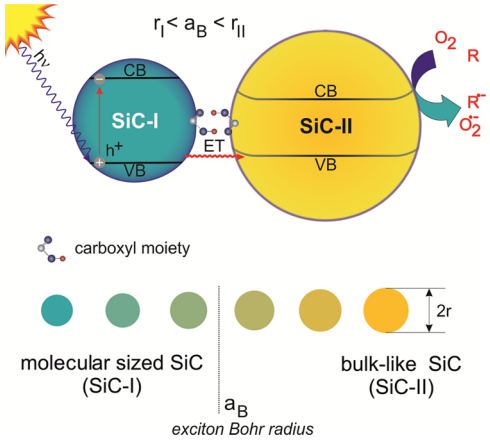

Figure 4. Proposed type I junction between two SiC NPs with different sizes. The difference in the band gaps allows charge separation and ET. a_B is the exciton Bohr radius, r is the radius of the SiC NP, and R stands for an organic group. VB and CB represent the valence and conduction bands or the occupied and the unoccupied energy levels, respectively.

is built up from materials with the same chemical composition in a colloid solution of uniformly charged particles. In other words, a type I homojunction is formed in the solution. We already demonstrated that wave functions of SiC NPs overlap when a thin film is created from SiC NPs.[22] It seems that such interaction is possible in solution, too. Furthermore, particle−particle interactions should be regulated by surface chemistry, as the surface groups determine the interaction between the particles. The major moieties on SiC NPs are the carboxyl groups and the hydroxyl groups after the synthesis; both are suitable for hydrogen bonding in aqueous solution. To study the effect of surface chemistry, we repeated the described experiments by using hydroxylated SiC NPs[40] by reducing the carboxyl surface moieties. Isolated hydroxylated SiC-I or SiC-II samples showed no differences in their photocatalytic efficiency compared to that of the samples before surface modification; however, if hydroxylated particles replaced either one of them or both SiC-I and SiC-II particles, the sensitizing effect did not appear in the mixed solution. This result implies that carboxyl groups play a major role in ET. Either hydrogen bonding between carboxyl moieties or interaction between the carboxyl and hydroxyl groups[45] in aqueous solution allows temporal cluster formation and subsequent ET.[46] However, the fact that the SiC-I and SiC-II particles are easily separated suggests that such particle−particle interaction should be weak.

CONCLUSIONS

We measured the photocatalytic properties of SiC NPs below 10 nm and found that SiC NPs of sizes between 1 and 4 nm do not have a photocatalytic activity. SiC NPs of sizes between 4 and 10 nm do have photocatalytic activity which is comparable to that of 100 nm ZnS NPs.

Size distribution and surface chemistry affect the overall efficiency of the system. As a result, SiC NP solutions with broad size distribution show surface-dependent photocatalytic activity as carboxylic-terminated SiC NPs exhibit higher performance than hydroxyl-terminated NPs do. Without separation, one can conclude that surface carboxyl groups cause significant enhancement to the photocatalytic efficiency. However, substitution of carboxyl moieties with hydroxyl groups does not affect the activity of the individual particles in the studied size range but changes the interaction between NPs that leads to dramatic change in the photocatalytic activity. Carboxyl-terminated SiC NPs with varying sizes tend to form temporary type I-like junctions enhancing the efficiency. Hydroxyl-terminated particles do not assemble; therefore, the sensitizing effect of the molecular-sized SiC NPs does not occur. Our result highlights the importance of surface moieties[47] in the photocatalytic activities of NPs beside the known geometry[48] as often organic molecules with carboxyl and hydroxyl groups are employed for colloid stabilization, but they may indirectly influence the overall photocatalytic efficiency of the entire solution via the varying ensemble formation of the NPs.

We also note that our results have implications on the biological applications of SiC NPs. We demonstrated that ultrasmall SiC NPs have no photoactivity; however, larger ones than 4 nm do, and the presence of larger particles can influence the viability tests or leads to an unwanted cell disease. However, proper regulation of the particle size and surface chemistry may open the door for programmed photoactivity in therapy.

ASSOCIATED CONTENT

Supporting Information

The Supporting Information is available free of charge on the ACS Publications website at DOI: 10.1021/acs.langmuir.7b03433.

Experimental details, instrumental, and additional figures (PDF)

AUTHOR INFORMATION

Corresponding Author

*E-mail: beke.david@wigner.mta.hu.

ORCID

David Beke: 0000-0001-6046-8164
Katalin Kamarás: 0000-0002-0390-3331
Adam Gali: 0000-0002-3339-5470

Author Contributions

The manuscript was written through contributions of all authors. All authors have given approval to the final version of the manuscript.

Funding

The authors would like to thank for the following research grants: NKFIH grant no. NVKP_16-1-2016-0152958, NK105691, TÁMOP-4.2.4.A/2-111/1-2012-00001 National Excellence Program, NTP-NFTÖ-16-0333, NTP-NFÖ-0052 National Talent Programs.

Notes

The authors declare no competing financial interest.

DOI: 10.1021/acs.langmuir.7b03433
Langmuir 2017, 33, 14263−14268

REFERENCES

(1) Herrmann, J. M. Heterogeneous photocatalysis: state of the art and present applications In honor of Pr. R.L. Burwell Jr. (1912−2003), Former Head of Ipatieff Laboratories, Northwestern University, Evanston (Ill). *Top. Catal.* **2005**, *34*, 49−65.

(2) Fujishima, A. Electrochemical Photolysis of Water at a Semiconductor Electrode. *Nature* **1972**, *238*, 37−38.

(3) Bahnemann, D. Photocatalytic Water Treatment: Solar Energy Applications. *Sol. Energy* **2004**, *77*, 445−459.

(4) Kubacka, A.; Fernández-García, M.; Colón, G. Advanced Nanoarchitectures for Solar Photocatalytic Applications. *Chem. Rev.* **2012**, *112*, 1555−1614.

(5) Dodd, A. C.; McKinley, A. J.; Saunders, M.; Tsuzuki, T. Effect of Particle Size on the Photocatalytic Activity of Nanoparticulate Zinc Oxide. *J. Nanopart. Res.* **2006**, *8*, 43−51.

(6) Mclaren, A.; Valdes-Solis, T.; Li, G.; Tsang, S. C. Shape and Size Effects of ZnO Nanocrystals on Photocatalytic Activity. *J. Am. Chem. Soc.* **2009**, *131*, 12540−12541.

(7) Li, J.; Wu, N. Semiconductor-Based Photocatalysts and Photoelectrochemical Cells for Solar Fuel Generation: A Review. *Catal. Sci. Technol.* **2015**, *5*, 1360−1384.

(8) Liqiang, J.; Yichun, Q.; Baiqi, W.; Shudan, L.; Baojiang, J.; Libin, Y.; Wei, F.; Honggang, F.; Jiazhong, S. Review of Photoluminescence Performance of Nano-Sized Semiconductor Materials and Its Relationships with Photocatalytic Activity. *Sol. Energy Mater. Sol. Cells* **2006**, *90*, 1773−1787.

(9) Wilker, M. B.; Schnitzenbaumer, K. J.; Dukovic, G. Recent Progress in Photocatalysis Mediated by Colloidal II-VI Nanocrystals. *Isr. J. Chem.* **2012**, *52*, 1002−1015.

(10) Holmes, M. A.; Townsend, T. K.; Osterloh, F. E. Quantum Confinement Controlled Photocatalytic Water Splitting by Suspended CdSe Nanocrystals. *Chem. Commun.* **2012**, *48*, 371.

(11) Wessling, B. Dissipative Structure Formation in Colloidal Systems. *Adv. Mater.* **1993**, *5*, 300−305.

(12) Yang, T.-C.; Chang, F.-C.; Peng, C.-Y.; Wang, H. P.; Wei, Y.-L. Photocatalytic Reduction of CO_2 with SiC Recovered from Silicon Sludge Wastes. *Environ. Technol.* **2015**, *36*, 2987−2990.

(13) White, J. L.; Baruch, M. F.; Pander, J. E., III; Hu, Y.; Fortmeyer, I. C.; Park, J. E.; Zhang, T.; Liao, K.; Gu, J.; Yan, Y.; Shaw, T. W.; Abelev, E.; Bocarsly, A. B. Light-Driven Heterogeneous Reduction of Carbon Dioxide: Photocatalysts and Photoelectrodes. *Chem. Rev.* **2015**, *115*, 12888−12935.

(14) van Dorp, D. H.; Hijnen, N.; Di Vece, M.; Kelly, J. J. SiC: A Photocathode for Water Splitting and Hydrogen Storage. *Angew. Chem., Int. Ed.* **2009**, *48*, 6085−6088.

(15) Zhu, F.; Hu, J.; Matulionis, I.; Deutsch, T.; Gaillard, N.; Kunrath, A.; Miller, E.; Madan, A. Amorphous Silicon Carbide Photoelectrode for Hydrogen Production Directly from Water Using Sunlight. *Philos. Mag.* **2009**, *89*, 2723−2739.

(16) Hao, J.-Y.; Wang, Y.-Y.; Tong, X.-L.; Jin, G.-Q.; Guo, X.-Y. Photocatalytic Hydrogen Production over Modified SiC Nanowires under Visible Light Irradiation. *Int. J. Hydrogen Energy* **2012**, *37*, 15038−15044.

(17) Gao, Y.; Wang, Y.; Wang, Y. Photocatalytic Hydrogen Evolution from Water on SiC under Visible Light Irradiation. *React. Kinet. Catal. Lett.* **2007**, *91*, 13−19.

(18) Schnabel, C.; Wörner, M.; González, B.; del Olmo, I.; Braun, A. M. Photoelectrochemical Characterization of P- and N-Doped Single Crystalline Silicon Carbide and Photoinduced Reductive Dehalogenation of Organic Pollutants at P-Doped Silicon Carbide. *Electrochim. Acta* **2001**, *47*, 719−727.

(19) Haibo, O.; Jianfeng, H.; Xierong, Z.; Liyun, C.; Cuiyan, L.; Xinbo, X.; Jie, F. Visible-Light Photocatalytic Activity of SiC Hollow Spheres Prepared by a Vapor−solid Reaction of Carbon Spheres and Silicon Monoxide. *Ceram. Int.* **2014**, *40*, 2619−2625.

(20) He, C.; Wu, X.; Shen, J.; Chu, P. K. High-Efficiency Electrochemical Hydrogen Evolution Based on Surface Autocatalytic Effect of Ultrathin 3C-SiC Nanocrystals. *Nano Lett.* **2012**, *12*, 1545−1548.

(21) Zhang, J.; Wu, X. L.; Liu, L. Z.; Yang, L.; Gan, Z. X.; Chu, P. K. 3C-SiC/ZnS Heterostructured Nanospheres with High Photocatalytic Activity and Enhancement Mechanism. *AIP Adv.* **2015**, *5*, 037120.

(22) Beke, D.; Szekrényes, Z.; Czigány, Z.; Kamarás, K.; Gali, Á. Dominant Luminescence Is Not due to Quantum Confinement in Molecular-Sized Silicon Carbide Nanocrystals. *Nanoscale* **2015**, *7*, 10982−10988.

(23) Hao, C.-H.; Guo, X.-N.; Pan, Y.-T.; Chen, S.; Jiao, Z.-F.; Yang, H.; Guo, X.-Y. Visible-Light-Driven Selective Photocatalytic Hydrogenation of Cinnamaldehyde over Au/SiC Catalysts. *J. Am. Chem. Soc.* **2016**, *138*, 9361−9364.

(24) Hong, J.; Meysami, S. S.; Babenko, V.; Huang, C.; Luanwuthi, S.; Acapulco, J.; Holdway, P.; Grant, P. S.; Grobert, N. Vertically-Aligned Silicon Carbide Nanowires as Visible-Light-Driven Photocatalysts. *Appl. Catal., B* **2017**, *218*, 267−276.

(25) Wang, B.; Wang, Y.; Lei, Y.; Wu, N.; Gou, Y.; Han, C.; Xie, S.; Fang, D. Mesoporous Silicon Carbide Nanofibers with in Situ Embedded Carbon for Co-Catalyst Free Photocatalytic Hydrogen Production. *Nano Res.* **2016**, *9*, 886−898.

(26) Beke, D.; Szekrényes, Z.; Pálfi, D.; Róna, G.; Balogh, I.; Maák, P. A.; Katona, G.; Czigány, Z.; Kamarás, K.; Rózsa, B.; Buday, L.; Vértessy, B.; Gali, A. Silicon Carbide Quantum Dots for Bioimaging. *J. Mater. Res.* **2013**, *28*, 205−209.

(27) Yang, L.; Zhao, H.; Fan, S.; Deng, S.; Lv, Q.; Lin, J.; Li, C.-P. Label-Free Electrochemical Immunosensor Based on Gold−Silicon Carbide Nanocomposites for Sensitive Detection of Human Chorionic Gonadotrophin. *Biosens. Bioelectron.* **2014**, *57*, 199−206.

(28) Somogyi, B.; Zólyomi, V.; Gali, A. Near-Infrared Luminescent Cubic Silicon Carbide Nanocrystals for in Vivo Biomarker Applications: An Ab Initio Study. *Nanoscale* **2012**, *4*, 7720−7726.

(29) Wu, R.; Zhou, K.; Yue, C. Y.; Wei, J.; Pan, Y. Recent Progress in Synthesis, Properties and Potential Applications of SiC Nanomaterials. *Prog. Mater. Sci.* **2015**, *72*, 1−60.

(30) Li, S.; Erickson, R. J.; Wallis, L. K.; Diamond, S. A.; Hoff, D. J. Modeling TiO2 Nanoparticle Phototoxicity: The Importance of Chemical Concentration, Ultraviolet Radiation Intensity, and Time. *Environ. Pollut.* **2015**, *205*, 327−332.

(31) Ibhadon, A. O.; Fitzpatrick, P. Heterogeneous Photocatalysis: Recent Advances and Applications. *Catalysts* **2013**, *3*, 189−218.

(32) Zhou, N.; López-Puente, V.; Wang, Q.; Polavarapu, L.; Pastoriza-Santos, I.; Xu, Q.-H. Plasmon-Enhanced Light Harvesting: Applications in Enhanced Photocatalysis, Photodynamic Therapy and Photovoltaics. *RSC Adv.* **2015**, *5*, 29076−29097.

(33) Waiskopf, N.; Ben-Shahar, Y.; Galchenko, M.; Carmel, I.; Moshitzky, G.; Soreq, H.; Banin, U. Photocatalytic Reactive Oxygen Species Formation by Semiconductor−Metal Hybrid Nanoparticles. Toward Light-Induced Modulation of Biological Processes. *Nano Lett.* **2016**, *16*, 4266−4273.

(34) Beke, D.; Szekrényes, Z.; Balogh, I.; Czigány, Z.; Kamarás, K.; Gali, A. Preparation of Small Silicon Carbide Quantum Dots by Wet Chemical Etching. *J. Mater. Res.* **2013**, *28*, 44−49.

(35) Mutschke, H.; Andersen, A. C.; Clement, D.; Henning, T.; Peiter, G. Infrared Properties of SiC Particles. *Astron. Astrophys.* **1999**, *345*, 187.

(36) Wieligor, M.; Wang, Y.; Zerda, T. W. Raman Spectra of Silicon Carbide Small Particles and Nanowires. *J. Phys.: Condens. Matter* **2005**, *17*, 2387−2395.

(37) Houas, A.; Lachheb, H.; Ksibi, M.; Elaloui, E.; Guillard, C.; Herrmann, J.-M. Photocatalytic Degradation Pathway of Methylene Blue in Water. *Appl. Catal., B* **2001**, *31*, 145−157.

(38) Alekseev, S.; Korytko, D.; Iazykov, M.; Khainakov, S.; Lysenko, V. Electrochemical Synthesis of Carbon Fluorooxide Nanoparticles from 3C-SiC Substrates. *J. Phys. Chem. C* **2015**, *119*, 20503−20514.

(39) Beke, D.; Károlyházy, G.; Czigány, Z.; Bortel, G.; Kamarás, K.; Gali, A. Harnessing No-Photon Exciton Generation Chemistry to Engineer Semiconductor Nanostructures. *Sci. Rep.* **2017**, *7*, 10599.

(40) Beke, D.; Jánosi, T. Z.; Somogyi, B.; Major, D. Á.; Szekrényes, Z.; Erostyák, J.; Kamarás, K.; Gali, A. Identification of Luminescence

DOI: 10.1021/acs.langmuir.7b03433
Langmuir 2017, 33, 14263−14268

Centers in Molecular-Sized Silicon Carbide Nanocrystals. *J. Phys. Chem. C* **2016**, *120*, 685−691.
(41) Chou, K.; Dennis, A. Förster Resonance Energy Transfer between Quantum Dot Donors and Quantum Dot Acceptors. *Sensors* **2015**, *15*, 13288−13325.
(42) Achermann, M.; Jeong, S.; Balet, L.; Montano, G. A.; Hollingsworth, J. A. Efficient Quantum Dot−Quantum Dot and Quantum Dot−Dye Energy Transfer in Biotemplated Assemblies. *ACS Nano* **2011**, *5*, 1761−1768.
(43) Samosvat, D. M.; Chikalova-Luzina, O. P.; Vyatkin, V. M.; Zegrya, G. G. Resonant Electronic Excitation Energy Transfer by Dexter Mechanism in the Quantum Dot System. *J. Phys.: Conf. Ser.* **2016**, *769*, 012078.
(44) Hoffman, J. B.; Choi, H.; Kamat, P. V. Size-Dependent Energy Transfer Pathways in CdSe Quantum Dot−Squaraine Light-Harvesting Assemblies: Förster versus Dexter. *J. Phys. Chem. C* **2014**, *118*, 18453−18461.
(45) Faure, B.; Salazar-Alvarez, G.; Ahniyaz, A.; Villaluenga, I.; Berriozabal, G.; De Miguel, Y. R.; Bergström, L. Dispersion and Surface Functionalization of Oxide Nanoparticles for Transparent Photocatalytic and UV-Protecting Coatings and Sunscreens. *Sci. Technol. Adv. Mater.* **2013**, *14*, 023001.
(46) Rogach, A. L.; Klar, T. A.; Lupton, J. M.; Meijerink, A.; Feldmann, J. Energy Transfer with Semiconductor Nanocrystals. *J. Mater. Chem.* **2009**, *19*, 1208−1221.
(47) Wu, C.-Y.; Tu, K.-J.; Deng, J.-P.; Lo, Y.-S.; Wu, C.-H. Markedly Enhanced Surface Hydroxyl Groups of TiO_2 Nanoparticles with Superior Water-Dispersibility for Photocatalysis. *Materials* **2017**, *10*, 566.
(48) Zhang, X.; Qin, J.; Xue, Y.; Yu, P.; Zhang, B.; Wang, L.; Liu, R. Effect of Aspect Ratio and Surface Defects on the Photocatalytic Activity of ZnO Nanorods. *Sci. Rep.* **2015**, *4*, 4596.

DOI: 10.1021/acs.langmuir.7b03433
Langmuir 2017, 33, 14263−14268